Article ID: 1003－6326(2005)02－0447－05

Modeling of velocity field for vacuum induction melting process①

CHEN Bo(陈 波), JIANG Zhi-guo(江治国), LIU Kui(刘 奎), LI Yi-yi(李依依)
(Institute of Metal Research, Chinese Academy of Sciences,
Shenyang 110016, China)

Abstract: The numerical simulation for the recirculating flow of melting of an electromagnetically stirred alloy in a cylindrical induction furnace crucible was presented. Inductive currents and electromagnetic body forces in the alloy under three different solenoid frequencies and three different melting powers were calculated, and then the forces were adopted in the fluid flow equations to simulate the flow of the alloy and the behavior of the free surface. The relationship between the height of the electromagnetic stirring meniscus, melting power, and solenoid frequency was derived based on the law of mass conservation. The results show that the inductive currents and the electromagnetic forces vary with the frequency, melting power, and the physical properties of metal. The velocity and the height of the meniscus increase with the increase of the melting power and the decrease of the solenoid frequency.

Key words: numerical simulation; electromagnetic force; molten alloy flow; free surface; induction melting
CLC number: TG 146.2; TG 249.4 **Document code:** A

1 INTRODUCTION

The alternating magnetic field can introduce motion in a molten metal without contacting the metal. In the steel industry, electromagnetic(EM) stirring is generally used to reduce inclusions, blowholes and other surface defects, while stirring beneath the crucible is aimed at minimizing segregation and homogeneities. The principal advantage of electromagnetic stirring is that it provides controlled stirring in any specific region in billet to influence metallurgical operations, such as dispersion and removal of inclusions and gas bubbles, in order to achieve particular metallurgical objectives. Experimental research on these aspects is limited due to the physical and chemical properties of the melts[1-6]. Most of prior researches have studied the continuous casting systems[7-11] and the surface wave on the free surface in a low frequency magnetic field[12, 13]. However, the frequency in the practical melting is always greater than 50 Hz, at which the fluid motion is not influenced by the body force oscillations due to its inertia[14], Davidson et al[15, 16] examined the flow in rotary stirring of round billets, and pointed that the induced flow in the billet was a superposition of the rotational flow driven by the applied rotating magnetic field and a secondary axial flow driven by the EM force gradient at the ends of the stirrer. Schwerdtfeger et al[17, 18] employed computational fluid dynamics techniques to investigate flow characteristics in rotary and vertical EM stirring of billets. The molten alloy has a high chemical activity and it will react with the stable crucible and the reaction speed highly depends on the operating parameters, namely, the frequency and magnitude of the induction coil current and geometry of the crucible on the flow. The impurity product will enter the molten alloy and the reaction speed mainly depends on the temperature and the velocity of the molten alloy, but the speed is difficult to measure in melting condition, so numerical simulation is always appealed to get the velocity field. Clearly, a detailed analysis of the flow in the EM stirred region of the molten pool is important to evaluate its effect on various metallurgical operations.

2 MODEL AND DERIVATION

The vacuum induction melt(VIM) furnace in the practice is schematically shown in Fig. 1. The heart of the furnace is the lime crucible (160 mm × 200 mm × 260 mm) surrounded by the coil connected a power supply, as illustrated in Fig. 2. The coil, billet and crucible are all rotationally symmetric and the rotational axis is y-axis, so the calculated domain is two-dimensional and half of the physical area.

The passage of AC current through the coils generates a traveling magnetic field in the system, which in turn induces currents in the steel billet. The interaction of the applied magnetic field with the induced current will give rise to an EM force field, which may drive the recirculating flow in the molten pool. The quantitative representation of electromagnetically driven flow in such systems re-

① **Received date:** 2004－12－06; **Accepted date:** 2005－01－18
Correspondence: CHEN Bo, PhD candidate; Tel: +86-24-23971983; E-mail: bchen@imr.ac.cn

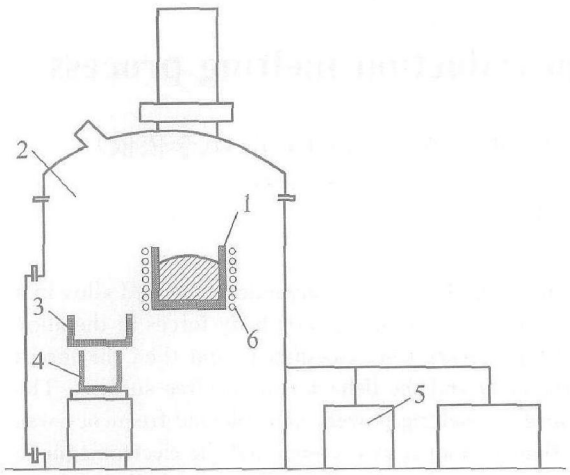

Fig. 1 Schematic diagram of VIM
1—Calcia crucible; 2—Vacuum chamber; 3—Tundish; 4—Mold; 5—Evacuating system; 6—Induction coil

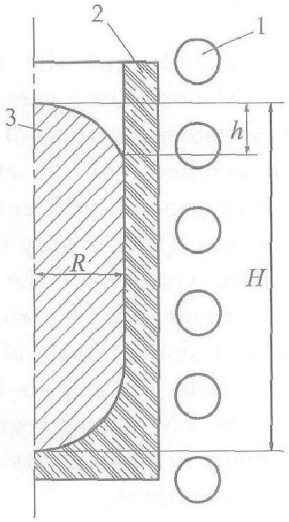

Fig. 2 Schematic diagram of calculated domain
1—Induction coil; 2—Lime crucible; 3—Molten metal

quires the solution of Maxwell's equations to calculate the electromagnetic field in the conducting region, and the solution of Navier-Stokes equation to calculate the flow driven by the EM force field.

At the wall of the crucible, the velocity of the molten metal is zero ($v_x = 0$, $v_y = 0$). The upper surface at the metal-vacuum interface is a free surface, where the press is zero ($p = 0$). At y-axis, the v_x is zero ($v_x = 0$).

The stirring hump is shown in Fig. 2. The height can be calculated from Eqn. (1):

$$h = \frac{F}{\gamma} = \frac{3.16 \times 10^{-2}}{\pi} \sqrt{\frac{\mu_r}{\rho \cdot f}} \cdot \frac{P}{d \cdot H \cdot \gamma} \quad (1)$$

where F is the magnetic force; h is the height of the hump in centimeters; γ is the density of the molten metal, kg/cm^3; μ_r is the relative magnetic conductivity; ρ is the resistance of the alloy, Ω/cm^{-2}; f is the coil frequency, Hz; P is the actual power, kW; d is the diameter of the crucible in centimeters; H is the height of the metal in centimeters.

If K is taken as $\frac{3.16 \times 10^{-2}}{\pi} \sqrt{\frac{\mu_r}{\rho}} \cdot \frac{1}{d \cdot \gamma}$, Eqn. (1) is transferred to Eqn. (2):

$$h = \frac{K \cdot P}{\sqrt{f} \cdot H} \quad (2)$$

We can get Eqn. (3) from Ref. [19]. R is the crucible radius in centimeters, M is the mass of the metal, kg. If m is taken as $\frac{M}{\rho \cdot \pi R}$, Eqn. (3) is transferred to Eqn. (4):

$$M = \rho \cdot \pi R^2 \cdot (H - \frac{h}{2}) \quad (3)$$

$$H = \frac{h}{2} + m \quad (4)$$

Eqn. (5) is obtained by Eqns. (2) and (4). And we can get Eqn. (6) from Eqn. (5):

$$h\left(\frac{h}{2} + m\right) = K \cdot \frac{P}{\sqrt{f}} \quad (5)$$

$$h = \sqrt{2K \frac{P}{\sqrt{f}} + m^2} - m \quad (6)$$

3 RESUTS AND DISCUSSION

It can be seen that if the solenoid frequency is decreased when melting a giving alloy, the inductive current can reach deeper position, and the magnetic stirring will perfect. Fig. 3 shows the magnetic forces of the molten metal on three different frequencies, namely 1.5, 2.5 and 4.0 kHz. the inductive current gets its max at the position of metal-crucible interface, and it attenuates rapidly in an exponential index with the depth increasing. The magnetic force gets its max at the same position as the place of current, and also attenuates rapidly also. The penetrating depth increases with the decreasing frequency. At 50 kW, when the frequency increases from 1.5 kHz to 4.0 kHz, the

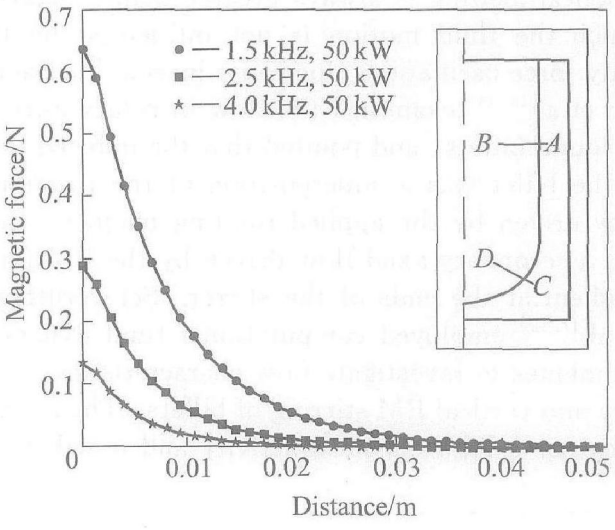

Fig. 3 Magnetic force distribution at 50 kW
(x-axis is distance to point C along line CD)

penetrated depth decreases to 60%. At 4.0 kHz, the skin effect is obvious and the penetrating depth is 1.0 cm, and the penetrating depths are respectively 1.3 cm and 1.6 cm when frequencies are 2.5 kHz and 1.5 kHz. The max inductive current is 1.3×10^7 A at 1.5 kHz, and 9.0×10^6 A at 4.0 kHz under 50 kW.

3.1 Effect of frequency

The magnetic force stirring at three different frequencies are calculated using the building model. The results are shown in Fig. 4. It is indicated that the velocity fields at three different frequencies are similar. There are two major circulation flow loops, and the upper is clockwise, another one is anticlockwise. The differences are the height of the meniscus and the speed of the velocity. The maximum speed flow is in the right-up position, which decreases from 0.59 m/s to 0.22 m/s as the frequency increases from 1.5 kHz to 4.0 kHz at 50 kW. Not only the velocity but also the height of the meniscus in the molten metal become smaller when the solenoid frequency increases from 1.5 kHz to 4.0 kHz.

The crucible is still and the velocity of the metal near the metal-crucible wall is assumed to be zero, but the magnetic force gets its max at the interface, so at a little distance away from the interface the metal is flowing. The reaction products between the alloy and the crucible can be transferred easily at the high velocity, which can cause severe erosion of the crucible. The velocity is different at different frequencies and different powers. It can be seen from the results that the melting power and solenoid frequency affect the velocity field. The lower the solenoid frequency is, the higher the velocity and meniscus height are. If velocity is 0.2 – 0.3 m/s, the reaction speed, the erodibility and the homogenization are all acceptable.

3.2 Effect of melting power

Similar to the effect of the frequency on velocity pattern, the higher the melting power is, the higher the computed velocity and meniscus height are. The magnetic force, the velocity and meniscus height are all increased with the increasing melting power. The flow patterns at different frequencies are computed. The result can be explained easily because the increasing power, the intensity magnetic field and the magnetic force all increase. Fig. 5 shows the velocity pattern at different melting powers. The highest speed is 0.25 m/s at 30 kW while it is 0.38 m/s at 70 kW under 2.5 kHz. From the simulation, the suitable velocity is obtained, i.e. 0.2 – 0.3 m/s. At this suitable velocity, we can get the homogenized alloy, and at the same time the crucible will erode only to a relatively slight extent. And we can get the suitable power and the suitable frequency through the suitable velocity.

3.3 Height of meniscus

From Eqn. (6), it can be seen that the height of the meniscus at the molten alloy surface varies with the solenoid frequencies, the melting powers, and the physical properties of the metal. From the simulated results the height of the meniscus at different frequencies and different melting powers are obtained. Fig. 6 shows the relationship be-

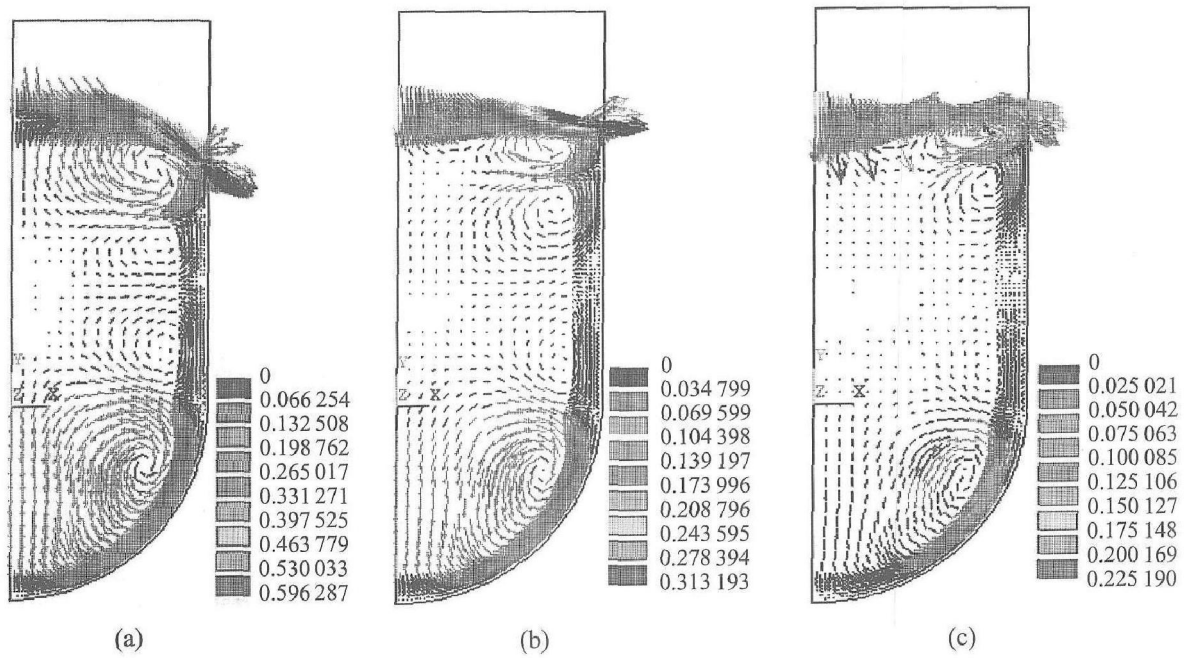

Fig. 4 Fields of velocity evolution at 50 kW
(a) —1.5 kHz; (b) —2.5 kHz; (c) —4.0 kHz

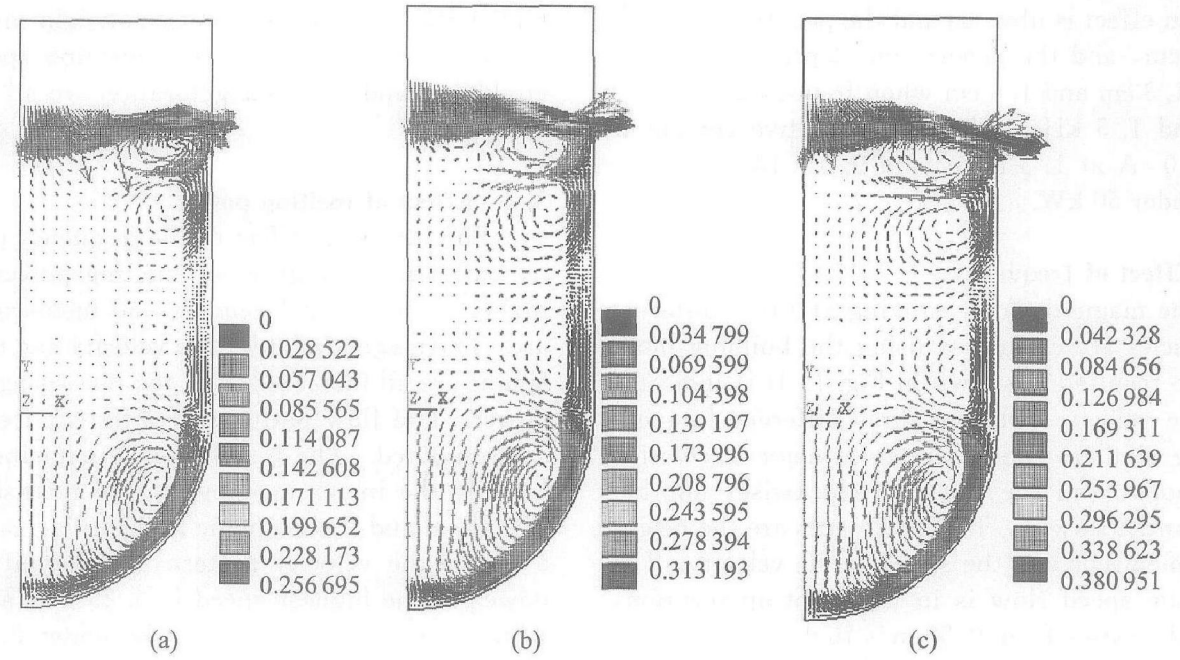

Fig. 5 Fields of velocity evolution at 2.5 kHz
(a) —30 kW; (b) —50 kW; (c) —70 kW

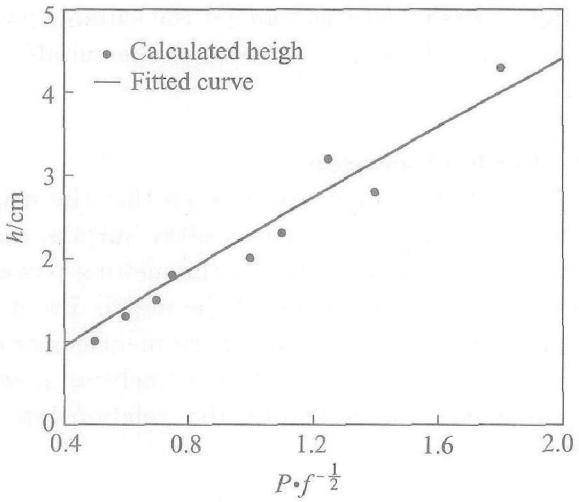

Fig. 6 Calculated height of meniscus and fitted curve
(K= 15, m= 5)

tween $P/\sqrt{f}$ and the height. The x-axis in the figure is $P/\sqrt{f}$ and y-axis is the height of the meniscus. Each dot in the figure represents one height at a frequency and a melting power. Fit the dots using Eqn. (6), then get the expression of Eqn. (7). The parameters in the function are K= 15 and m= 5. The expression is shown as follows:

$$h = \sqrt{30\frac{P}{\sqrt{f}} + 25} - 5 \quad (7)$$

Eqn. (7) shows that the height increases with the increase of the melting power and with the decrease of the solenoid frequency.

4 CONCLUSIONS

1) A mathematical model is built to simulate the electromagnetic field and velocity field in the melting metal. The surface behavior is also described.

2) The magnetic force increases with the increasing melting power and the decreasing solenoid frequency. The intensity and depth exponential attenuate with the increasing distance away from the surface.

3) There are two major circulations flow loops. The melting power and frequency affect the speed of flow and the height of surface meniscus. The higher power (or lower frequency) is, the higher the computed velocity and height are.

4) The height of surface meniscus is the function of the melting power and frequency, and it can be expressed as $h = \sqrt{30\frac{P}{\sqrt{f}} + 25} - 5$.

REFERENCES

[1] Li T, Nagaya S, Sassa K, et al. Study of meniscus behavior and surface properties during casting in a high-frequency magnetic field [J]. Metall Mater Trans B, 1995, 26B: 353-359.

[2] Schwarze R, Obermeier F. Modelling of unsteady electromagnetically driven recirculating melt flows [J]. Modelling Simul Mater Sci Eng, 2004, 12: 985-993.

[3] Szekely J, Chang C W. Electromagnetically driven flows in metals processing [J]. J Metals, 1976, 28: 6-11.

[4] Spalart P R. Strategies for turbulence modelling and simulations [J]. Int J Heat Fluid Flow, 2000, 21: 252-263.

[5] El-Kaddah N, Szekely J, Taberlet E, et al. Turbulent recirculating flows in induction furnaces: a comparison

of measurements with predictions over a range of operating conditions [J]. Metall Trans B, 1986, 17B: 687 - 693.

[6] Yao Y F, Savill A M, Sandham N D, et al. Simulation and modelling of turbulent trailing-edge flow [J]. Flow Turbul Combust, 2002, 68: 313 - 333.

[7] Meyer J L, Szekely J, El-Kaddah N. Calculation of the electromagnetic force field for induction stirring in continuous casting [J], Trans ISIJ, 1987, 27: 25 - 33.

[8] Kubo N, Ishii T, Kubota J, et al. Numerical simulation of molten steel flow under a magnetic field with argon gas bubbling in a continuous casting mold [J]. ISIJ Int, 2004, 44(3): 556 - 564.

[9] Natarajan T T, El-Kaddah N. Finite element analysis of electromagnetically driven flow in sub-mold stirring of steel billets and slabs [J]. ISIJ Int, 1998, 38: 680 - 689.

[10] Catalano P, Wang M, Iaccarino G, et al. Numerical simulation of the flow around a circular cylinder at high reynolds numbers [J]. Int J Heat Fluid Flow, 2003, 24: 463 - 469.

[11] Solorio-diaz G, Morales R D, Palafax-ramos J, et al. Analysis of fluid flow turbulence in tundishes fed by a swirling ladle shroud [J]. ISIJ Int, 2004, 44(6): 1024 - 1032.

[12] Tarapore E D, Evans J W. Fluid velocities in induction melting furnaces(part Ⅰ) —theory and laboratory experiments [J]. Metall Trans B, 1976, 7B: 343 - 351.

[13] Tarapore E D, Evans J W. Fluid velocities in induction melting furnaces(part Ⅱ) —large scale measurement and predictions [J]. Metall Trans B, 1977, 8B: 179 - 184.

[14] Felten F, Fautrelle Y, Du-Terrail Y, et al. Numerical modelling of electromagnetically-driven turbulent flows using LES methods [J]. Applied Mathematical Modelling, 2004, 28: 15 - 27.

[15] Davidson P A, Boysan F. The importance of secondary flow in the rotary electromagnetic stirring of steel during continuous casting [J]. Appl Sci Res, 1987, 44: 241 - 259.

[16] Davidson P A. Electromagnetic stirring of steel and aluminum [A]. Magnetohydrodynamics in Process Metallurgy, the Metallurgical Society [C]. Warrendale: PA, 1992. 241 - 249.

[17] Dubke M, Tacke K, Spitzer K, et al. Flow fields in electromagnetic stirring of rectangular strand with linear inductor(part Ⅰ) —theory and experiments with cold models [J]. Metall Trans B, 1988, 19B: 581 - 594.

[18] Dubke M, Tacke K, Spitzer K, et al. Flow fields in electromagnetic stirring of rectangular strand with linear inductor(part Ⅱ) —computation of flow fields in billets, blooms and slabs of steel [J]. Metall Trans B, 1988, 19B: 595 - 602.

[19] SU Yang-qing, LIU Yuan, GUO Jing-jie, et al. Molding of temperature field for the induction skull melting process of Ti-47Ni-9Nb [J]. Metall Mater Trans A, 2001, 32A: 2895 - 2902.

(Edited by LI Xiang-qun)